

This is an electronic appendix to the paper by Alun L. Lloyd 2001
Destabilization of epidemic models with the inclusion of realistic dis-
tributions of infectious periods. *Proc. R. Soc. Lond. B* **268**, 985-993.

Electronic appendices are refereed with the text. However, no attempt has been
made to impose a uniform editorial style on the electronic appendices.

1 Alternative Formulations of the Model

As discussed in the main text, the inclusion of non-exponential distributions means that the chance of recovery depends on the time since infection, and hence the model needs to keep track of this information. The main text discusses how the method of stages can be used to incorporate a gamma-distributed infectious period within the SIR framework. Here, we discuss two alternative formulations, namely the integro-differential equation formulation and the partial differential equation formulation.

In the integro-differential equation formulation, we describe the infectious period distribution by the probability density function $f(\tau)$. This density function can be integrated to give the survivorship function,

$$F^s(y) = \int_y^\infty f(\tau) d\tau \quad (1)$$

which gives the probability that an individual remains in the infectious class for at least y time units, given that they have not first died. Notice that the survivorship function is one minus the cumulative density function corresponding to $f(\tau)$.

The probability that an individual infected τ time units ago recovers in the time interval $(\tau, \tau + d\tau)$ is $f(\tau)d\tau$. Since the infection rate τ time units previously was $\beta S(t - \tau)I(t - \tau)$, the rate at which individuals recover is

$$\int_0^\infty \beta S(t - \tau)I(t - \tau)f(\tau)e^{-\mu\tau} d\tau. \quad (2)$$

The factor $e^{-\mu\tau}$ takes infective mortality into account. Notice that in the special case in which all individuals have exactly the same duration of infection, so that $f(\tau)$ is a delta function, expression (2) reduces to a simple delay term; the individuals who recover now are precisely those who were infected $1/\gamma$ time units ago and have not yet died.

In the partial differential equation approach, the infective class is labelled with the time since infection, τ , so that the number of individuals who have been infectious for between τ and $\tau + d\tau$ time units is $I(t; \tau)d\tau$. The dynamics of the infective class is described by the partial differential equation

$$\frac{\partial}{\partial t} I(t; \tau) + \frac{\partial}{\partial \tau} I(t; \tau) = -F(\tau)I(t; \tau) - \mu I(t; \tau) \quad (3)$$

together with the initial condition

$$I(t; 0) = \int \beta S(t)I(t; \tau)d\tau. \quad (4)$$

This partial differential equation (3) is entirely familiar from age-structured models (see, for example, Anderson & May 1991), with the left hand side expressing the total derivative of I with respect to time (for each individual τ increases at the same rate as t) and the right hand side expressing the recovery rate of individuals who have been infected for τ time units and the natural mortality of infectives. The initial condition (4) describes the infection process; the overall rate of infection at time t is simply the product of the total number of infectives, as given by the integral, the number of susceptibles and the transmission parameter. The function $F(\tau)$ is known as the hazard function, and standard results (see, for example, Cox & Miller 1965) show that it is related to the survivorship function by

$$F(\tau) = f(\tau)/F^s(\tau), \quad (5)$$

or equivalently

$$dF^s(\tau)/d\tau = -F(\tau)F^s(\tau). \quad (6)$$

Notice that it would be particularly simple within this formulation to model a situation in which an individual's infectiousness varied over the infectious period by allowing the transmission parameter to be dependent on τ .

Both of these formulations are more difficult to study analytically or to simulate numerically than the stage formulation on which we focus in the main text.

2 Details of Bifurcation Analysis of the Forced Model

As mentioned in the text, because of the large swings in the number of infective individuals in the seasonally forced model, we found that the numerical bifurcation analysis was facilitated by transforming the state variables of the model onto a logarithmic scale. For the standard SIR model, if one defines $X = \ln S$ and $Y = \ln I$, use of the results $dX/dt = (dS/dt)/S$ and $dY/dt = (dI/dt)/I$ show that the logged variables satisfy the following set of ODEs

$$\frac{dX}{dt} = \mu N \exp(-X) - \beta(t) \exp(Y) - \mu \quad (7)$$

$$\frac{dY}{dt} = \beta(t) \exp(X) - (\mu + \gamma). \quad (8)$$

Given the initial conditions $(S(0), I(0))$, this set of equations can then be integrated over one year to give $(S(1), I(1))$, thus defining the time-one map discussed in the text. The logarithmic transformation can be applied in a similar way to the n stage model.

The numerical bifurcation analysis requires estimates for the derivatives of the time-one map. In the non-forced case (with constant $\beta(t)$), these can be obtained directly from the partial derivatives (i.e. the Jacobian matrix) of the functions appearing on the right hand sides of equations (7) and (8). In the forced case, standard results can be used to derive an equation for the time evolution of a perturbation made to a known trajectory.

We consider a set of initial conditions $(X(0), Y(0))$, whose time evolution is described by $(X(t), Y(t))$. We perturb the initial conditions by $(x(0), y(0))$, where $(x(0), y(0))$ is small, and write the trajectory which results from this perturbed initial condition as $(X(t)+x(t), Y(t)+y(t))$. Writing down the equations for the time evolution of the unperturbed and perturbed trajectories, subtracting and then ignoring quadratic and higher order terms in the small quantities $x(t)$ and $y(t)$, it is easy to see that

$$\begin{pmatrix} dx/dt \\ dy/dt \end{pmatrix} = Df_{(X(t), Y(t))} \begin{pmatrix} x(t) \\ y(t) \end{pmatrix}. \quad (9)$$

The Jacobian matrix again describes the time evolution of perturbations, but this matrix itself is time-varying. This equation cannot be solved analytically in the general case, so we evaluate the partial derivatives of the time-one map by integrating equation (9) numerically over the course of one year. Since equation (9) is linear in the perturbations, this is a more reliable way of obtaining estimates of the partial derivatives of the time-one map than numerical differentiation of the time-one map itself.

3 Formulation and Analysis of the SEIR Model

The traditional SEIR model (see, for instance, Anderson & May 1991) includes an exposed, but not yet infectious, class of individuals, accounting for a latent period between an infection event and an individual becoming infectious. In the standard model, this latent period is described by an exponential distribution of average duration $1/\sigma$ (i.e., if the number of exposed individuals is

written as E , then the term in describing the movement of individuals from the exposed to the infectious class is $-\sigma E$).

More generally, the latent period can be described by a probability density function, $g(\tau)$, which gives the probability of an individual infected τ time units ago becoming infectious in the time interval $(\tau, \tau + d\tau)$ as $g(\tau) d\tau$. As with the distribution of infectious periods, this can be integrated to give a survivorship function, $G^s(y)$. We fix the average duration of the latent period to be $1/\sigma$, as in the basic model.

The expression for the basic reproductive number, R_0 , is similar to that derived for the general SIR model, except for the appearance of an extra factor which expresses the probability that an individual will pass through the exposed class and become infectious. This probability is one minus the probability of the individual dying during the latent period and is therefore approximately equal to one, unless the duration of the latent period is significant compared to the average lifespan. We have

$$R_0 = \frac{\beta N}{\mu} H(\mu) \{1 - G(\mu)\}, \quad (10)$$

where G is the integral defined by equation (9) in the main text, and H is the corresponding integral with the function f being replaced by g (see also Hethcote & Tudor 1980).

The values of S and I at the endemic equilibrium are given by the same expressions as for the SIR model, but with the value of R_0 just given. Equilibrium stability analysis is easily performed and leads to the following expression for the dominant eigenvalue

$$(\Lambda + \mu) + \beta I^* - \beta S^* H(\Lambda + \mu) \{1 - G(\Lambda + \mu)\} = 0. \quad (11)$$

As before, we have explicit expressions for G and H in the case of gamma distributed latent and infectious periods, and we can then solve equation (11) numerically.

Figure 1 shows the damping time of the endemic equilibrium as a function of both the number of infective stages, n , and the number of exposed stages, m , for latent periods of different lengths, varying from much shorter than the infectious period (figure 1a), through the same length as the infectious period (figure 1b), to much longer than the infectious period (figures 1c and 1d).

As discussed in the main text, if the latent phase is much shorter than the infectious period, i.e. $\sigma \gg \gamma$, then the SEIR model behaves much like the corresponding SIR model, and we see destabilization of the equilibrium when more realistic distributions of the infectious period are employed, just as we saw in the SIR case (figure 1b in the main text). Notice that when the latent phase is short compared to the infectious period, then changing its distribution has little effect on the damping time.

We see that when the latent phase is of a similar duration to the infectious period (figure 1b), the damping time need not be an increasing function of the number of infective stages, although this is only observed here for the exponentially distributed exposed class and notice that the damping time of the more realistic model is still greater than that of the basic model. The damping time is a increasing function of the number of exposed classes; more realistic distributions of the exposed class lead to destabilization of the equilibrium.

With longer latent phases (figures 1c and 1d), the damping time can be a decreasing function of n , although this most commonly observed for the smaller values of m . As might be expected, when the infectious period is short compared to the latent phase, changing the distribution of infectious periods has little effect on equilibrium stability.

Although not as clear-cut as the SIR case presented in the main text, the main conclusion that can be drawn from the stability analysis of the endemic equilibrium is that destabilization occurs when both latent and infectious period distributions become less dispersed.

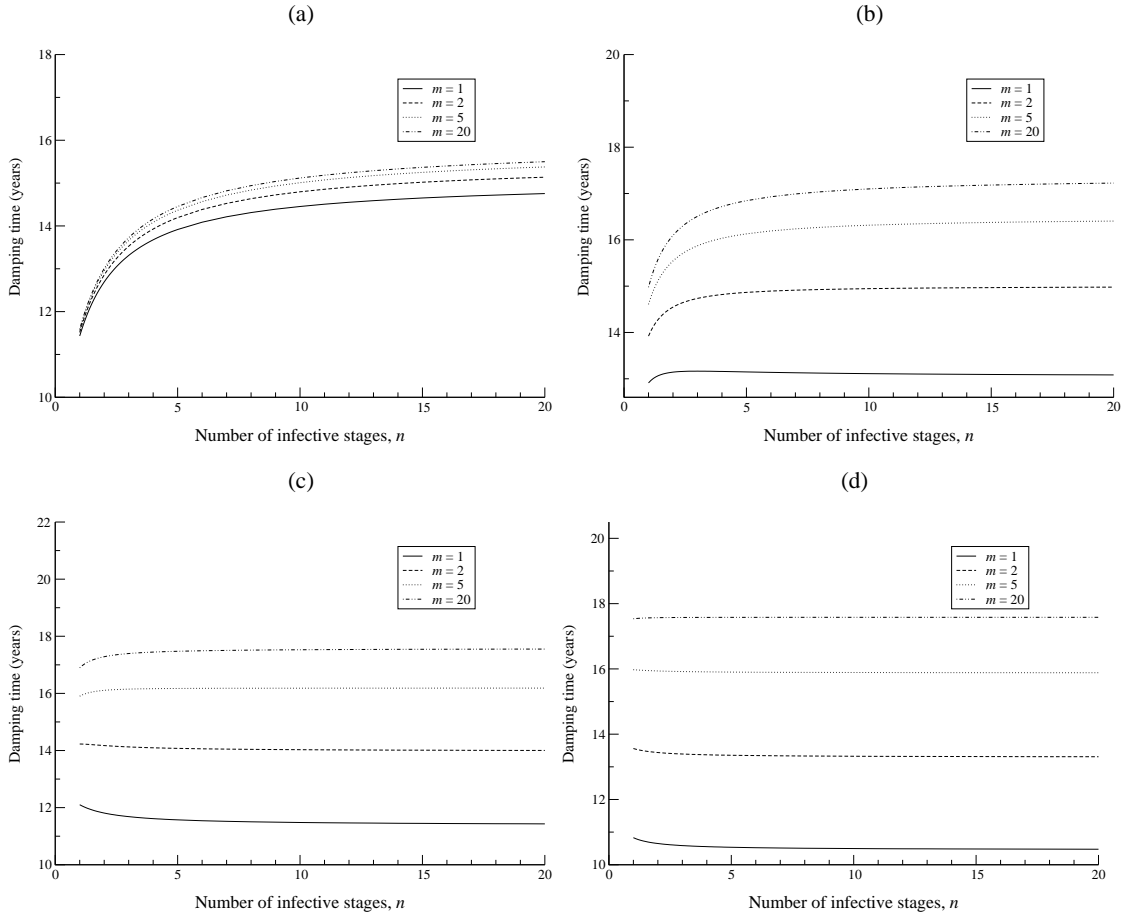


Figure 1: Stability of the endemic equilibrium of the general SEIR model, as measured by the damping time, with varying numbers of infective stages (n) and either one, two, five or twenty exposed stages (m). Parameter values used in the model are $N = 10^7$ individuals, $\beta = 1000/N$ individual⁻¹year⁻¹, $\gamma = 100 \text{ year}^{-1}$ and $\mu = 1/50 \text{ year}^{-1}$. Results are illustrated for various lengths of the latent period: (a) short latent period, $\sigma = 500 \text{ year}^{-1}$, (b) latent period equal to the infectious period, $\sigma = 100 \text{ year}^{-1}$, and long latent periods (c) $\sigma = 35 \text{ year}^{-1}$ and (d) $\sigma = 10 \text{ year}^{-1}$.

4 Destabilization of the Seasonally Forced SEIR Model

With the introduction of seasonal variations in the contact rate, the SEIR model undergoes multi-annual oscillations. As for the SIR case, bifurcation analysis can be used to study the changing nature of these oscillations as system parameters are varied. Here we compare the basic SEIR model to one with five infectious and five exposed stages, with a latent period chosen to be roughly three times longer compared to the infectious period. This parameter value was chosen for two reasons: firstly, because the long latent period makes the model less like the SIR model studied in the main text, and secondly to enable comparison with the results of Kuznetsov & Piccardi (1994).

Figures 2a and 2b show various bifurcations affecting annual and biennial oscillations. As noted by Kuznetsov & Piccardi (1994), the bifurcation diagram of the SEIR model is somewhat simpler than of the corresponding SIR model since several of the bifurcations seen in figures 3a and 3b of the main text are not seen within the parameter range illustrated here. Again notice the correspondence between figures 2a and 2b, together with the general trend of destabilization.

To summarize these results, figure 3 shows the strength of seasonality required to achieve biennial oscillations in the basic SEIR model compared to the more realistic one, and as was seen in the SIR case, biennial oscillations are achieved with lower levels of seasonality in the more realistic model.

5 References

Anderson, R.M., & May, R.M. 1991 *Infectious Diseases of Humans: Dynamics and Control*. Oxford: Oxford University Press.

Cox, D.R., & Miller, H.D. 1965 *The Theory of Stochastic Processes*. Chapman & Hall: London.

Hethcote, H.W., & Tudor, D.W. 1980 Integral equation models for endemic infectious diseases. *J. Math. Biol.* **9**, 37-47.

Kuznetsov, Y.A., & Piccardi, C. 1994 Bifurcation analysis of periodic SEIR and SIR epidemic models. *J. Math. Biol.* **32**, 109-121.

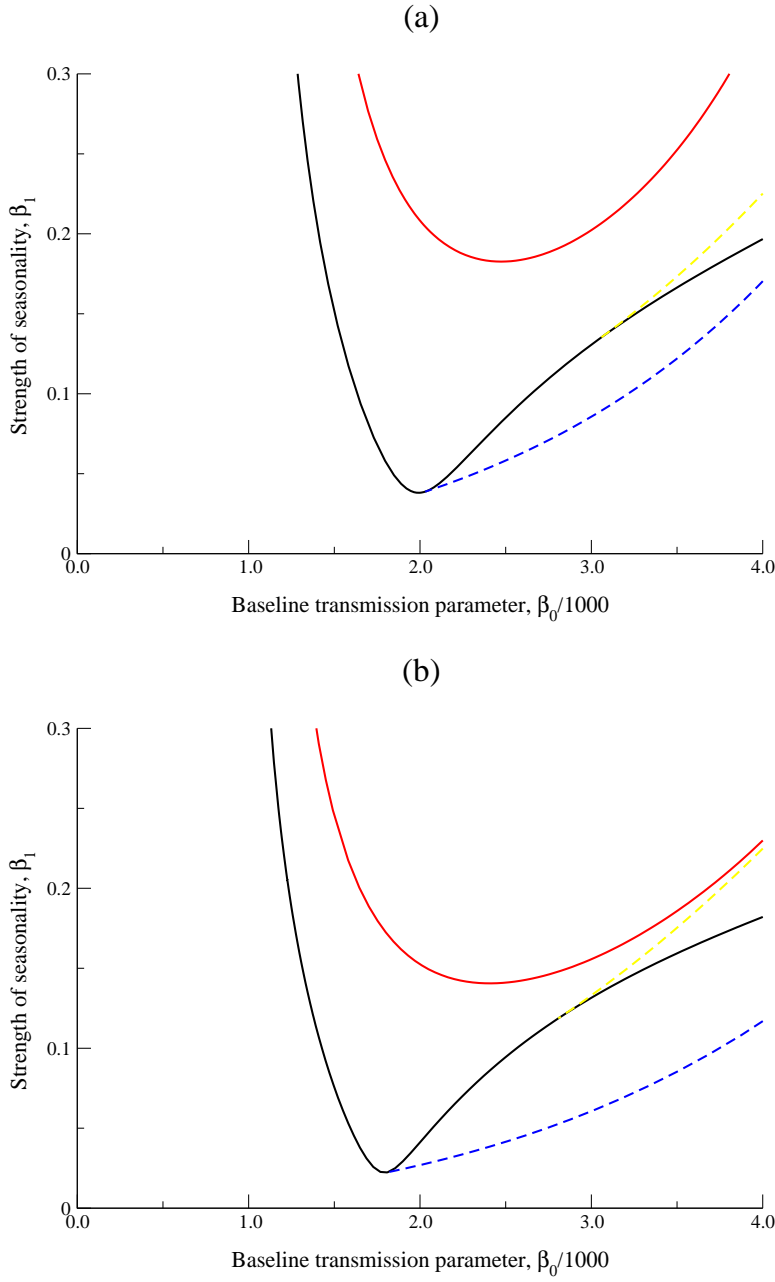


Figure 2: Bifurcation diagrams for the seasonally forced SEIR model. (a) basic model, $n = m = 1$ and (b) more realistic model $n = m = 5$. Parameter values used are $\beta = 1000/N$ individual⁻¹year⁻¹, $\gamma = 100$ year⁻¹, $\sigma = 35.842$ year⁻¹ and $\mu = 1/50$ year⁻¹. The colours and line-styles of the curves are as in figure 3 of the main text. Solid lines represent period doubling (flip) bifurcations, dashed lines represent tangent (saddle-node) bifurcations. The black curve traces out the parameter values at which period doubling of the annual cycle occurs. The dashed blue curve, which meets the black curve at its minimum, denotes the set of parameter values at which a tangent bifurcation creates a pair of biennial cycles. The yellow dashed curved denotes another set of tangent bifurcations involving biennial cycles, and the red curve denotes period doubling of biennial cycles.

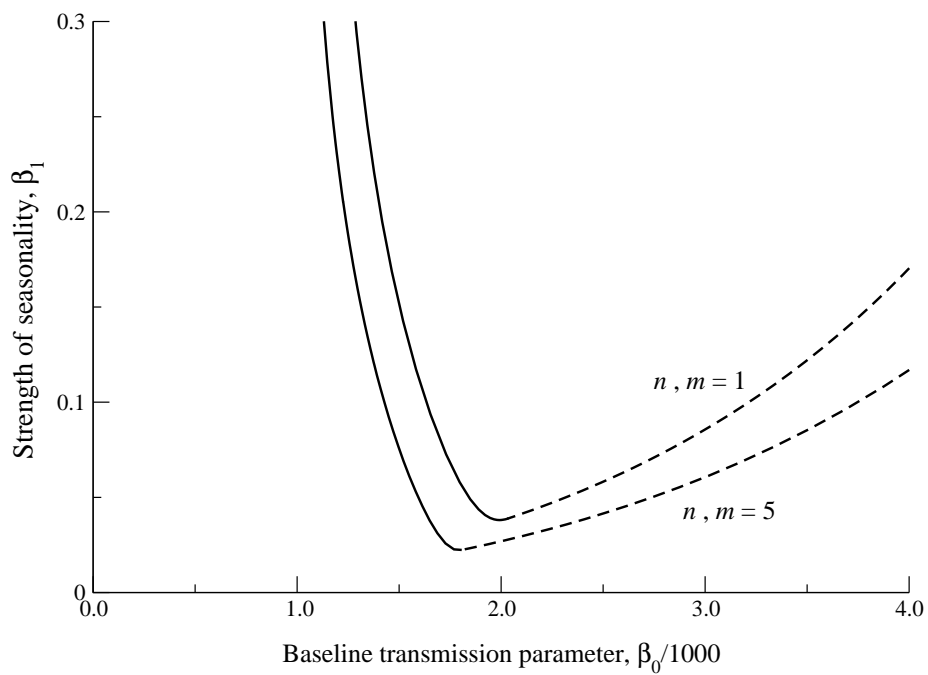


Figure 3: The strength of seasonality required to generate biennial cycles in the basic ($n = m = 1$) and more realistic ($n = m = 5$) models, for a range of values for the baseline rate of transmission (or, rescaling the axis, R_0). As before, we indicate parameter ranges for which the biennial cycles are first generated by the period doubling (solid curve) or tangent (broken curve) bifurcations. Parameter values as in figure 2.